Applied Surface Science 337 (2015) 1–5

Contents lists available at ScienceDirect

Applied Surface Science

journal homepage: www.elsevier.com/locate/apsusc

Interfacial scanning tunneling spectroscopy (STS) of chalcogenide/metal hybrid nanostructure

Mahmoud M. Saad[a], Tamer Abdallah[a], Khalid Easawi[b], Sohair Negm[b], Hassan Talaat[a,*]

[a] Physics Department, Faculty of Science, Ain Shams University, Abbassia, Cairo, Egypt
[b] Department of Physics and Mathematics, Faculty of Engineering (Shoubra), Benha University, Egypt

ARTICLE INFO

Article history:
Received 8 July 2014
Received in revised form
31 December 2014
Accepted 20 January 2015
Available online 11 February 2015

Keywords:
Scanning tunneling spectroscopy
Metal chalcogenide interfaces
Interfacial band bending

ABSTRACT

The electronic structure at the interface of chalcogenide/metal hybrid nanostructure (CdSe–Au tipped) had been studied by UHV scanning tunneling spectroscopy (STS) technique at room temperature. This nanostructure was synthesized by a phase transfer chemical method. The optical absorption of this hybrid nanostructure was recorded, and the application of the effective mass approximation (EMA) model gave dimensions that were confirmed by the direct measurements using the scanning tunneling microscopy (STM) as well as the high-resolution transmission electron microscope (HRTEM). The energy band gap obtained by STS agrees with the values obtained from the optical absorption. Moreover, the STS at the interface of CdSe–Au tipped hybrid nanostructure between CdSe of size about 4.1 ± 0.19 nm and Au tip of size about 3.5 ± 0.29 nm shows a band bending about 0.18 ± 0.03 eV in CdSe down in the direction of the interface. Such a result gives a direct observation of the electron accumulation at the interface of CdSe–Au tipped hybrid nanostructure, consistent with its energy band diagram. The presence of the electron accumulation at the interface of chalcogenides with metals has an important implication for hybrid nanoelectronic devices and the newly developed plasmon/chalcogenide photovoltaic solar energy conversion.

1. Introduction

Recently, the advancement in fabrication of semiconductor/metal (S/M) hybrid nanostructures opens new opportunities for designing multifunctional materials with properties that cannot be obtained in the bulk phase. The electronic properties of S/M contact on a nanoscale are fundamental and intriguing problems [1] since understanding the properties of such nanocontacts is important for usage in nanoelectronic devices and other applications in the photovoltaic solar energy conversion. In the semiconductor bulk regime, the interface is characterized by the space-charge region. Feenstra and Martensson [2] observed the band bending at the interface between a monolayer of Sb on p-type GaAs using the scanning tunneling spectroscopy (STS). In the nanoregime, the interface region is comparable to the hybrid nanoparticle's size; therefore, the concepts should be reinvestigated. Smit and coworkers [3] proposed a model to describe the potential barrier shape in S/M nanocontact, and concluded that the barrier thickness decreases with decreasing the size. Landman et al. [4] studied the nanocontacts formed between Si nanowires (few nm long) and Al nanoelectrodes. They predicted the induction of subgap states near the Si–Al interface that rapidly decay into the Si. Steiner and coworkers [5] used low temperature UHV scanning tunneling spectroscopy (STS) to probe the electronic structure of CdSe–Au nanodumbbell. In our work, an organic synthesis method was used for preparation of CdSe quantum dots (QDs), and a phase transfer chemical method for tipping the gold (Au) on these quantum dots to obtain CdSe–Au tipped hybrid nanostructure. Our interest lies in the interfacial electronic structure of chalcogenide/metal hybrid nanostructure. We used room temperature UHV Omicron STM for STS to investigate the interfacial electronic structure of this hybrid nanostructure, and the measurements were initiated by the drop casting method. Few drops of the colloidal solution of the sample were spread on a flat conducting substrate. As the solvent evaporates, the nanoparticles gently touch the conducting substrate. In STS, a change of the voltage bias results in an equal change of the tip Fermi level with respect to energy levels of the nanoparticles while the Fermi level of the substrate remains unchanged [6]. In this asymmetrical configuration (substrate–nanoparticle–vacuum gap–tip), there are no linker molecules between the substrate and nanoparticles, so the tip

* Corresponding author at: Physics Department, Ain Shams University, Khalifa Elmaamoon Street, Abbassia, Cairo, Egypt. Tel.: +20 24854254; fax: +20 24842560.
E-mail address: hassantalaat@hotmail.com (H. Talaat).

http://dx.doi.org/10.1016/j.apsusc.2015.01.152
0169-4332/

Fermi level scans over the energy levels of the nanoparticle. At a positive sample bias, the onset of the differential of the current with respect to the voltage biasing $dI/dV > 0$ indicates the resonant tunneling from the tip to the substrate via a discrete unoccupied level in the conduction band (CB). At a negative sample bias, the onset of $dI/dV > 0$ corresponds to the resonant tunneling from the substrate to the tip via a discrete occupied level in the valance band (VB). Therefore, it is possible to derive the band gap from the region around zero bias of the tunneling spectra, in which dI/dV is close to zero [7]. The fine structures of the electron and hole levels at room temperature are hard to detect.

The band gap measured by STS is employed through the corrected effective mass approximation model (corrected EMA) [8–10] to calculate the size of chalcogenide nanoparticles (NPs), and compared to the direct measurement of the dimensions of chalcogenide NPs from the STM image. In the corrected EMA model, the electron–hole coulomb potential is ignored, and the energy band gap of the nanocrystals (NC) E_g^{NC} is given by Eq. (1).

$$E_g^{NC} = E_g^{Bulk} + \frac{h^2\pi^2}{2mD^2}, \quad (1)$$

where E_g^{Bulk} is the bulk band gap energy, D is the diameter of the nanoparticle, m is the reduced mass of the electron and the hole, and h is the Planck's constant.

On the other hand, the UV–vis absorption is also used to obtain the exciton and the plasmon absorption peaks. The band gap of chalcogenide NPs can be calculated from $E_g^{NC} = hc/\lambda_{max}$, where λ_{max} is the wavelength at the maximum of the exciton absorption peak, and c is the velocity of light. The effective mass approximation model (EMA) [11] is further used to calculate the size of chalcogenide NPs. In the EMA model, the energy band gap E_g^{NC} including the electron–hole coulomb potential is given by Eq. (2).

$$E_g^{NC} = E_g^{Bulk} + \frac{h^2\pi^2}{2mD^2} - \frac{1.8e^2}{2\pi\varepsilon\varepsilon_0 D}, \quad (2)$$

where ε_0 is the permittivity of free space, ε is the permittivity of the chalcogenide, e is the electron charge, and $1.8e^2/(2\pi\varepsilon\varepsilon_0 D)$ is the electron–hole coulomb part.

2. Materials and experimental procedures

2.1. Preparation of cadmium selenide (CdSe) quantum dots (QDs) nanoparticles

A 0.3 g of cadmium oxide (CdO, Aldrich) was dissolved in 2 g stearic acid at 170 °C, and then a mixture of 2 g of TOPO and 2 g of HDA was added and held at 180 °C for 5 min to get a clear solution. The resultant solution was kept warm and stored in a syringe to use as a cadmium (Cd) source. A 0.3 g of selenium (Se) was dissolved in 6 mL of trioctylphosphine (TOP, Fluka), then stored in another syringe to use as a source. This solution was quickly injected into the prepared Cd source, and the reaction mixture was raised to 130 °C for the growth of CdSe QDs [12].

2.2. Preparation of CdSe–Au tipped hybrid nanoparticles (NPs)

A 5 mL of octylamine was injected into 15 mL of CdSe QDs solution, and the resulting mixture was sonicated for 20 s before precipitating with methanol. The solution was then centrifuged at 5000 rpm for 10 min. The colorless supernatant was decanted off, and the above process was repeated several times. The precipitate was then re-dispersed in toluene maintaining a concentration of 0.06 mg/mL, a part of which (~5 mL) was then stirred with 10^{-4} M aqueous $HAuCl_4$. Aliquots of the top toluene layer were separated from the biphasic mixture after 30 min [13].

2.3. Technical measurements

Optical absorption spectra of nanosamples were recorded using Ocean Optics spectrophotometer. Sizes and shapes of the synthesized NPs were determined using JEOL JEM-2100LaB_6 high-resolution transmission electron microscope (HRTEM) operated at 200 kV and equipped with Gatan bottom CCD camera. UHV Omicron scanning tunneling microscope (STM) was used for topography and spectroscopy at room temperature. The tip height was set using a gap voltage of +0.2 V, a feedback current of 1 nA and a loop gain of 50%. The STM topography was performed by scanning over 400 lines and 400 points. In the scanning tunneling spectroscopy (STS), we applied a sample bias range of [−2 V, +2 V], a delay time of 50 μs and an acquisition time of 160 μs.

3. Results and discussions

The UV–vis absorption spectra of CdSe QDs before and after Au tipping are shown in Fig. 1. The exciton absorption peak of CdSe QDs is about 514 nm. The corresponding average particle size calculated by EMA equation with the bulk band gap E_g (bulk) for CdSe as 1.74 eV [14] were about 4.2 nm. The additional peak around 535 nm, appearing in the CdSe–Au tipped absorption spectrum, is due to the localized surface plasmon (LSP) of the gold tip [15].

The HRTEM image of CdSe QDs is shown in Fig. 2a. The measured average size of CdSe NPs presented in the figure is about 4.3 ± 0.8 nm. Fig. 2b shows an enlarged HRTEM image of CdSe NP surrounded by the dashed circle presented in Fig. 2a. The measured interplanar spacing of CdSe of about 0.34 nm is consistent with the literature [16].

Fig. 3a shows the STM image of CdSe QDs, where the average particle size is about 4.0 ± 0.2 nm for the selected particles indicated by (x). Fig. 3b shows the average STS of the six indicated CdSe NPs. The Fermi level position is at 0 V. The conduction band edge E_C is at +1.31 V and the valence band edge E_V is at −1.31 V, so the measured band gap of the CdSe QDs is about 2.62 eV with a symmetrical form around 0 V bias as an intrinsic semiconductor. Furthermore, the average particle size was also calculated using the band gap as obtained by STS from Fig. 3b and the corrected EMA equation discussed above, which gave a value of 4.1 ± 0.15 nm as the average diameter. This calculated particle size is in full agreement with the directly measured average given by the STM image, and is close to the values measured by the HRTEM image.

The HRTEM image of CdSe–Au tipped hybrid nanosample is shown in Fig. 4a. The measured average size of CdSe NPs is about 4.5 ± 0.6 nm, and the Au tip average size is about 2.9 ± 0.8 nm. Fig. 4b shows an enlarged HRTEM image of CdSe–Au tipped hybrid NP. The measured Au tip interplanar spacing of about 0.22 nm is consistent with the literature [17].

In order to study the electronic structure at the interface of the Au tip on the CdSe NP, the STS tunneling spectra were measured at three different regions. These regions are A (the Au tip), B (CdSe NP away from the Au tip) and C (close to the edge of the Au tip). Such assignments were done after we had carried out the measurement of the STS tunneling spectra, and were determined according to the shape of the resulting STS tunneling spectra. The region giving STS curve around the zero bias with a narrow band width was assigned to be (A). Region B was determined from the symmetric STS curve resulting from the measurement on CdSe NP away from the Au tip. The asymmetric measured curve, assigned to region C, would be at the interface between the edge of the Au tip and the CdSe NP. Fig. 5a shows a schematic diagram of CdSe–Au tipped NP. Fig. 5b shows STM image of CdSe–Au tipped NPs. the Au tip assigned by (A) is about 3.5 ± 0.29 nm and the size of the assigned CdSe–Au tipped NP is about 4.1 ± 0.19 nm. Fig. 5c shows the corresponding

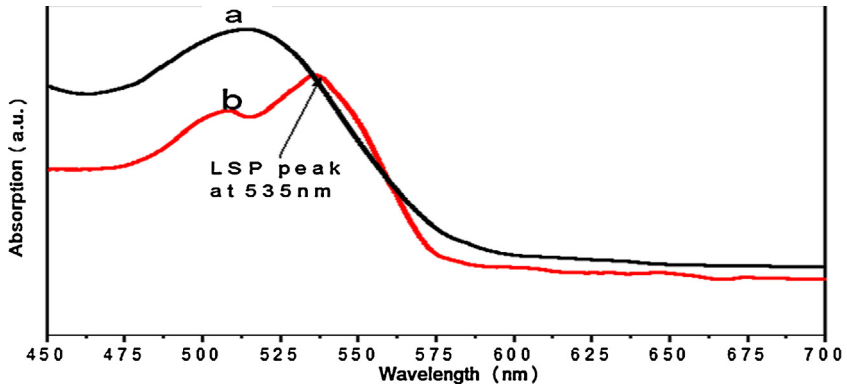

Fig. 1. UV–vis absorption spectra of (a) CdSe QDs, and (b) CdSe–Au tipped hybrid nanosample.

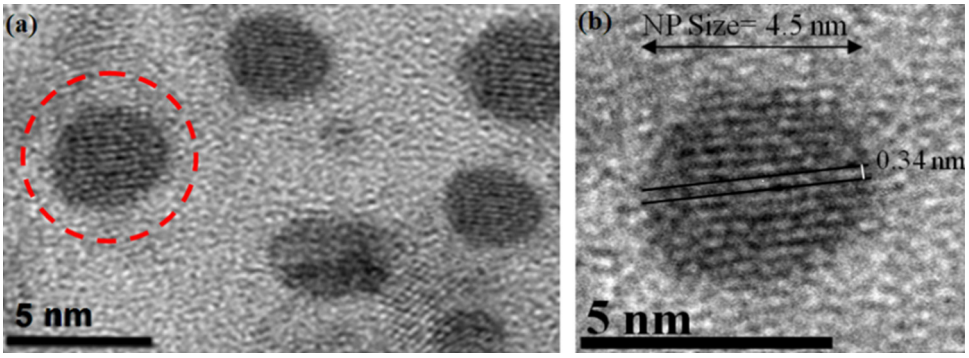

Fig. 2. (a) HRTEM image of CdSe QDs, and (b) an enlarged HRTEM image of CdSe NP that is surrounded by the dashed circle.

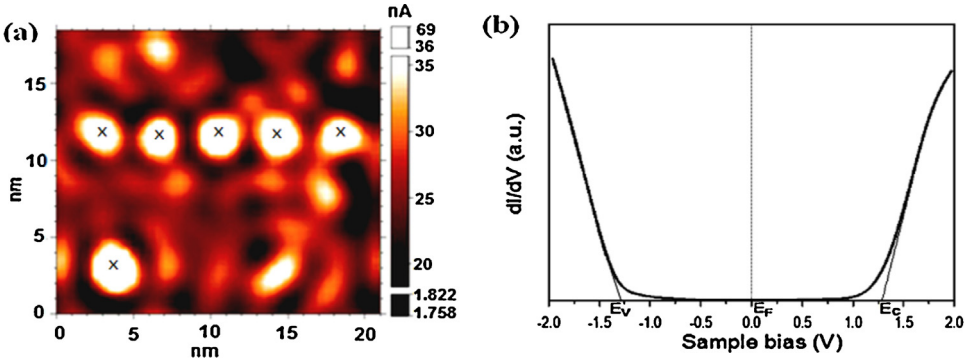

Fig. 3. (a) STM image of CdSe QDs, and (b) the corresponding STS average tunneling spectrum for the selected CdSe NPs indicated by (x). The valence band and conduction band edges are denoted by E_V and E_C respectively. The Fermi level E_F corresponds to 0 V.

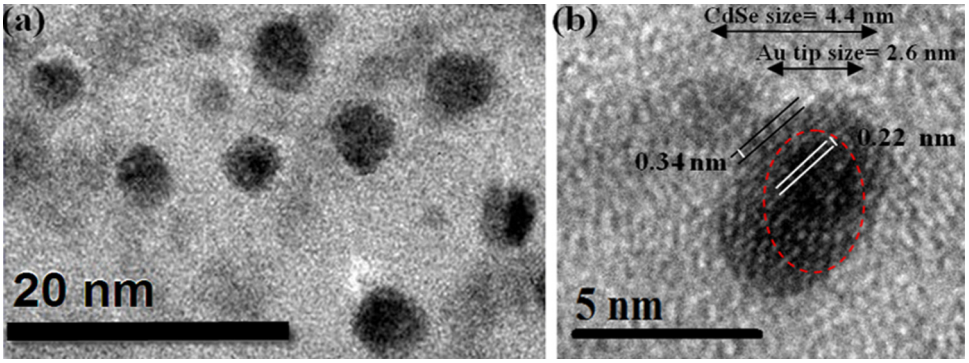

Fig. 4. (a) HRTEM image of CdSe–Au tipped hybrid nanosample, and (b) an enlarged HRTEM image of CdSe–Au tipped hybrid NP. The surrounded area by the dashed circle represents the Au tip position as determined from the image contrast and the interplanar spacing values.

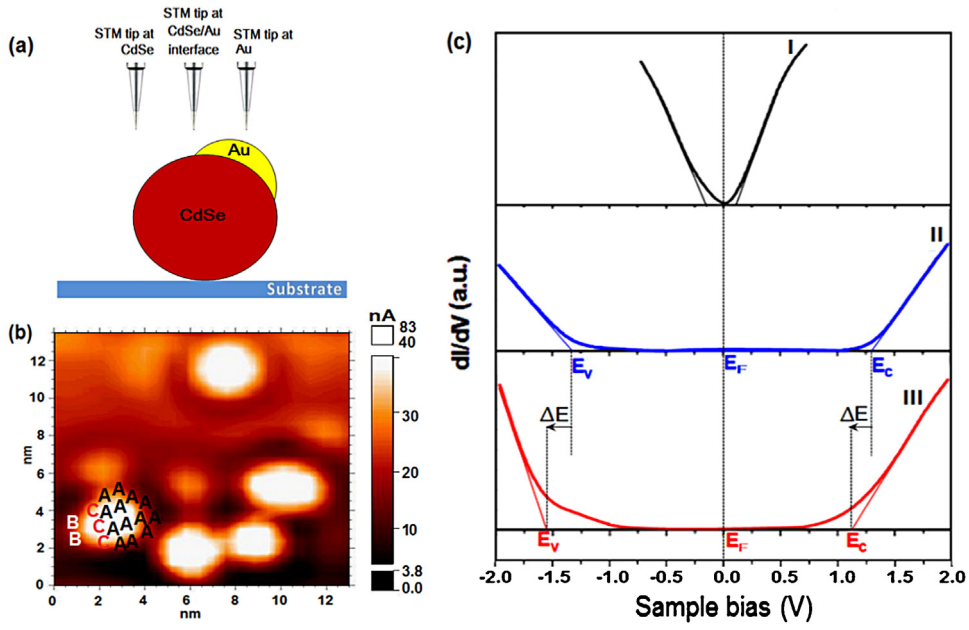

Fig. 5. (a) A schematic diagram of CdSe–Au tipped, (b) STM image of CdSe–Au tipped, in which region A is the Au tip location, region B is CdSe away from the Au tip, and region C is close to the edge of Au tip, and (c) corresponding STS tunneling spectra along a single particle of CdSe–Au tipped at the three regions. Curve I is at region A, curve II is at region B, and curve III is at region C. The conduction band and valence band edges are denoted by E_C and E_V respectively. The Fermi level E_F corresponds to 0 V.

STS tunneling spectra I, II and III at the three regions A, B and C respectively. The STS tunneling spectra were obtained at each point indicated in the figure, and were averaged for each region.

Curve I in Fig. 5c represents the STS at the Au tip position (region A), and shows a coulomb blockade [18] about 0.23 eV as measured between the intercepts of the positive and the negative tangents of the curve. In Curve II, measured on CdSe away from the Au tip (region B), E_C is at +1.31 V and E_V is at −1.31 V. The measured band gap of the CdSe QDs is about 2.62 eV as an intrinsic semiconductor with a symmetrical form around 0 V bias, and gives the same value as obtained for CdSe NPs presented above. In curve III, acquired close to the edge of Au tip (region C), E_C is at +1.16 V and E_V is at −1.52 V, so the measured band gap is about 2.68 eV with an asymmetrical form around 0 V bias. The difference in the value of the measured band gap of the CdSe QD between curve II and curve III may be attributed to a difference in dimensionality at these points of measurements of the CdSe QD. In the kinematics of STS measurement, the Fermi level E_F of the sample always appears at 0 V bias, so the average 0.18 ± 0.03 eV negative shift ΔE of the band edges E_C and E_V shown in curve III relative to curve II is due to the positive energy shift of the Fermi level toward equilibrium between the CdSe QD and the Au tip. This shift causes a down band bending toward the interface by the same amount. Consequently, it can be concluded that there is an accumulation of electrons at the interface.

A model of the electronic energy band diagram of CdSe of size about 4.1 nm and Au tip of size about 3.5 nm before and after contact are shown in Fig. 6a and b respectively. The dimensions were selected to be coincident with the values measured from the STM image of CdSe–Au tipped. The bulk electron affinity of CdSe was taken as 4.95 eV [14]. A CdSe NP of size about 4.1 nm has a band gap about 2.62 eV and an electron affinity about 4.26 eV. The Au tip ionization potential *(IP)* was calculated using the formula proposed by Halas [19]

$$IP = W_\infty + \frac{3}{8} \cdot \frac{e^2}{2\pi\varepsilon_0 D}, \tag{3}$$

where W_∞ is the bulk work function of Au, which is taken as 5.1 eV [20], and D is the size of Au tip measured as 3.5 nm. Before contact as shown in Fig. 6a, the Fermi level of Au tip is aligned at −5.41 eV relative to the vacuum level, and the Fermi level of the intrinsic CdSe NP, aligned at the middle of the band gap, is at −5.57 eV. On contact as shown in Fig. 6b, the Fermi level of CdSe shifts by about 0.16 eV toward the conduction band edge to reach equilibrium, causing a band bending down in the direction of the interface by this amount.

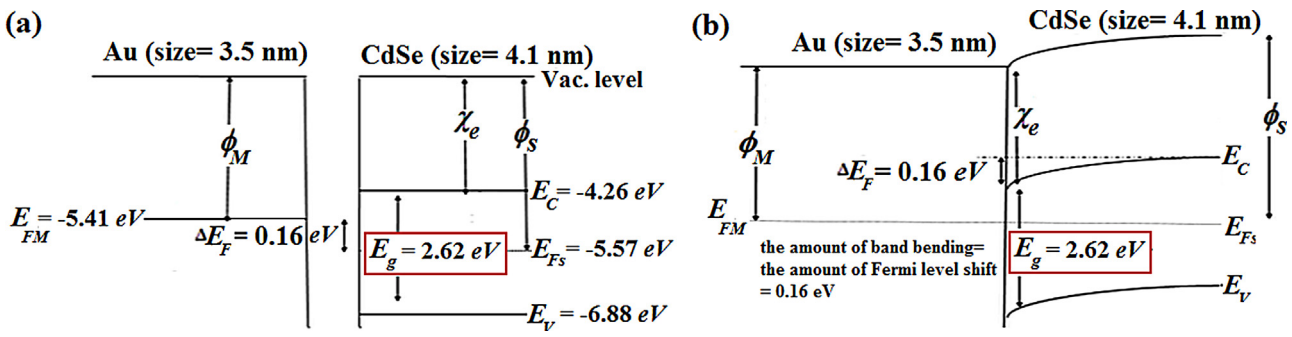

Fig. 6. A model of the electronic energy band diagram of CdSe QD of size 4.1 nm and Au tip of size 3.5 nm (a) before contact and (b) after contact.

Table 1
Sizes and band gaps of CdSe QDs before and after Au tipping.

Sample	CdSe size (nm)				CdSe band gap (eV)	
	Optical absorption and EMA	HRTEM image	STM image	STS	Optical absorption	STS
CdSe	4.2 ± 0.01	4.3 ± 0.8	4.0 ± 0.2	4.1 ± 0.15	2.4 ± 0.01	2.62 ± 0.08
CdSe–Au tipped	4.3 ± 0.01	4.5 ± 0.6	4.1 ± 0.19	3.9 ± 0.13	2.4 ± 0.01	2.68 ± 0.04

Such a result is in agreement with the result obtained from the STS presented in Fig. 5c-III.

Table 1 shows a summary of the comparison between the results of sizes and band gaps of CdSe QDs before and after Au tipping as obtained from the optical absorption, HRTEM, STM and STS. The sizes of CdSe NPs obtained from the optical absorption using the EMA model are in close agreement with the direct measurements using HRTEM as well as STM. The metal tip dimensions, measured from the STM images, were confirmed by the direct measurements of HRTEM. Furthermore, band gaps obtained from the optical absorption are also in good agreement with the values measured by STS.

4. Conclusion

CdSe–Au tipped hybrid nanostructure has been used for studying the interfacial electronic structure of chalcogenide/metal contact in the nanoregime. The electronic bands of CdSe bend down in the direction of the interface as a result of the Fermi level equilibration between the CdSe NP and the Au tip. This shift in the band edges was detected experimentally from the asymmetry in STS at the interface between the CdSe NP and the Au tip. Such a result gives a clear evidence for the existence of the electron accumulation at the interface of CdSe–Au tipped hybrid nanostructure. The presence of the electron accumulation at the interface of chalcogenides with metals has an important implication in plasmon-quantum dot synthesized solar cells.

Acknowledgment

The generous support of the Egyptian SDTF grant ID 377 is greatly appreciated.

References

[1] R. Costi, A.E. Saunders, U. Bani, Angew. Chem. 49 (2010) 4878–4897.
[2] R.M. Feenstra, P. Martensson, Phys. Rev. Lett. 61 (1988) 447.
[3] G.D.J. Smit, S. Rogge, T.M. Klapwijk, Appl. Phys. Lett. 81 (2002) 3852.
[4] U. Landman, R.N. Barnett, A.G. Scherbakov, P. Avouris, Phys. Rev. Lett. 85 (2000) 1958.
[5] D. Steiner, T. Mokari, U. Banin, O. Millo, Phys. Rev. Lett. 95 (2005) 056805.
[6] A. Many, Y. Goldstein, N.B. Grover, Semicond. Surf. (1965).
[7] H. Talaat, T. Abdallah, M.B. Mahmed, S. Negm, M.A. El-Sayed, Chem. Phys. Lett. 473 (2009) 288–292.
[8] L. Efros, M. Rosen, Annu. Rev. Mater. Sci. 30 (2000) 475.
[9] D.S. Chemla, D.A.B. Miller, Opt. Lett. 11 (1986) 522.
[10] E.A. Muljarov, et al., Phys. Rev. B 62 (2000) 7420.
[11] W.W. Yu, L. Qu, W. Guo, X. Peng, Chem. Mater. 15 (2003) 2854–2860.
[12] K. Easawi, M. Nabil, T. Abdallah, S. Negm, H. Talaat, Proc. World Acad. Sci. Eng. Technol. 61 (2012) 548–551.
[13] T. Bala, A. Singh, A. Sanyal, C. O'Sullivan, F. Laffir, C. Coughlan, M. Ryan, Nano Res. 6 (2013) 121–130.
[14] J. Wang, M. Isshiki, Springer Handbook of Electronic and Photonic Materials, 2007, pp. 325–342.
[15] M. Fox, Optical Properties of Solids, 2nd ed., 2010.
[16] P. Hu, D. Jia, Y. Cao, Y. Huang, L. Liu, J. Luo, Nanoscale Res. Lett. (2009).
[17] J. Torresdey, J. Parsons, E. Gomez, J. Videa, H. Troiani, P. Santiago, M. Yacaman, Nano Lett. 2 (2002) 397–401.
[18] W. Hanson, Fundamentals of Nanoelectronics, 2007.
[19] S. Halas, Chem. Phys. Lett. 370 (2003) 300–301.
[20] CRC Handbook of Chemistry and Physics version, 2008.